

# Influence of the Valley Degeneracy on Spin Relaxation in Thin Silicon Films

Dmitry Osintsev<sup>1,2</sup>, Viktor Sverdlov<sup>1</sup>, and Siegfried Selberherr<sup>1</sup>

<sup>1</sup> Institute for Microelectronics, TU Wien, Gußhausstraße 27-29/E-360, 1040 Wien, Austria

<sup>2</sup> Volgograd State Technical University, Lenin Avenue 28, 400131 Volgograd, Russia

E-mail: {Osintsev|Sverdlov|Selberherr}@iue.tuwien.ac.at

**Abstract**— Semiconductor spintronics is a rapidly developing field with a potentially large impact on microelectronics. Using electron spin may help to reduce power consumption and increase computational speed of modern electronic circuits. Silicon is perfectly suited for spin-based applications: it is characterized by a weak spin-orbit interaction which should result in a long spin lifetime. However, recent experiments indicate the lifetime may get significantly reduced in gated structures. Thus, understanding the peculiarities of the subband structure and details of the spin propagation in surface layers and thin silicon films in presence of the spin-orbit interaction is urgently needed. We investigate the contribution of the spin-orbit interaction to the equivalent valley splitting and calculate the spin relaxation matrix elements by using a perturbative  $\mathbf{k} \cdot \mathbf{p}$  approach. We demonstrate that the valley degeneracy strongly influences the spin relaxation matrix elements. Shear strain is an efficient concept to lift the valley degeneracy, which can considerably suppress the electron spin relaxation in silicon surface layers and thin films.

*Spin relaxation in silicon;  $k \cdot p$  method; spin-orbit interaction; shear strain; surface roughness*

## I. INTRODUCTION

Various devices utilizing spin properties of electrons have already been proposed [1], [2]. Silicon is the basic element of modern microelectronics. At the same time silicon possesses several properties attractive for spin-driven applications: it is composed of nuclei with predominantly zero spin and it is characterized by weak spin-orbit coupling. However, large experimentally observed spin relaxation in electrically-gated silicon structures may become an obstacle in realizing spin driven devices [3], and a deeper understanding of fundamental spin relaxation mechanisms in silicon is urgently needed [4].

We investigate the influence of the intrinsic spin-orbit interaction on the spin relaxation matrix elements due to surface roughness in silicon-on-insulator (SOI) films. To accurately describe the band structure in the presence of the intrinsic spin-orbit interaction a  $\mathbf{k} \cdot \mathbf{p}$  Hamiltonian [5], [6] has been generalized to include the spin degree of freedom [7]. The spin-orbit coupling produces a large mixing of the spin-up and spin-down states between the two unprimed degenerate subbands, resulting in spin

“hot spots” characterized by strong spin relaxation. Shear strain is able to efficiently lift the degeneracy between the unprimed subbands [6], which should substantially improve the spin lifetime in gated silicon structures.

## II. MODEL

We numerically investigated the dependences of the matrix elements due to surface roughness induced spin relaxation in silicon films as a function of shear strain. For [001] oriented valleys in a (001) silicon film the Hamiltonian is written in the vicinity of the  $X$  point along the  $k_z$ -axis in the Brillouin zone. The basis is conveniently chosen as  $[(X_1, \uparrow), (X_1, \downarrow), (X_2, \uparrow), (X_2, \downarrow)]$ , where  $\uparrow$  and  $\downarrow$  indicate the spin projection at the quantization  $z$ -axis. The effective  $\mathbf{k} \cdot \mathbf{p}$  Hamiltonian reads as

$$H = \begin{bmatrix} H_1 & H_3 \\ H_3^\dagger & H_2 \end{bmatrix}, \quad (1)$$

where  $H_1$ ,  $H_2$ , and  $H_3$  are written as

$$H_1 = \left[ \frac{\hbar^2 k_z^2}{2m_l} - \frac{\hbar^2 k_0 k_z}{m_l} + \frac{\hbar^2 (k_x^2 + k_y^2)}{2m_t} + U(z) \right] I, \quad (2)$$

$$H_2 = \left[ \frac{\hbar^2 k_z^2}{2m_l} + \frac{\hbar^2 k_0 k_z}{m_l} + \frac{\hbar^2 (k_x^2 + k_y^2)}{2m_t} + U(z) \right] I, \quad (3)$$

$$H_3 = \begin{bmatrix} D\epsilon_{xy} - \frac{\hbar^2 k_x k_y}{M} & (k_y - k_x i)\Delta_{SO} \\ (-k_y - k_x i)\Delta_{SO} & D\epsilon_{xy} - \frac{\hbar^2 k_x k_y}{M} \end{bmatrix}. \quad (4)$$

Here  $m_t$  and  $m_l$  are the transversal and the longitudinal silicon effective masses,  $k_0 = 0.15 \times 2\pi/a$  is the position of the valley minimum relative to the  $X$ -point in unstrained silicon,  $\epsilon_{xy}$  denotes the shear strain component,  $M^{-1} \approx m_t^{-1} - m_0^{-1}$ ,  $U(z)$  is the confinement potential, and  $D = 14\text{eV}$  is the shear strain deformation potential. The spin-orbit term  $\tau_y \otimes (k_x \sigma_x - k_y \sigma_y)$  with

$$\Delta_{so} = \frac{\hbar^2}{2m_0^3 c^2} \left| \sum_n \frac{\langle x_1 | p_j | n \rangle \langle n | [\nabla V \times p]_j | x_2 \rangle}{E_n - E_X} \right|, \quad (5)$$

couples states with the opposite spin projections from the opposite valleys.  $\sigma_x$  and  $\sigma_y$  are the spin Pauli matrices and  $\tau_y$  is the  $y$ -Pauli matrix in the valley degree of freedom,  $c$  is the speed of light, and  $\otimes$  is the symbol for the matrices direct product. We found the value  $\Delta_{SO} = 1.27\text{meV nm}$  close to the one reported in [7].

In the presence of strain and confinement the four-fold degeneracy of the  $n$ -th unprimed subband is partly lifted by forming an  $n+$  and  $n-$  subladders (the valley splitting), however, the degeneracy of the eigenstates with the opposite spin projections  $|n\pm\uparrow\rangle$  and  $|n\pm\downarrow\rangle$  within each subladder is preserved.

The degenerate states are chosen to satisfy

$$\langle \uparrow n \pm | f | n \pm \downarrow \rangle = 0, \quad (6)$$

with the operator  $f$  defined as

$$f = \cos \theta \sigma_z + \sin \theta (\cos \varphi \sigma_x + \sin \varphi \sigma_y), \quad (7)$$

where  $\theta$  is the polar and  $\varphi$  is the azimuth angle defining the orientation of the injected spin. In general, the expectation value of the operator  $f$  computed between the spin up and down states from different subladders is nonzero, when the effective magnetic field direction due to the spin-orbit interaction is different from the injected spin quantization axis

$$\bar{f} = \langle \uparrow n \pm | f | \mp n \downarrow \rangle \neq 0. \quad (8)$$

### III. RESULTS AND DISCUSSION

#### A. Valley splitting calculations

First we investigate the value of the energy splitting between the subbands with the same quantum number  $n$  but from different subsets  $n+$  and  $n-$  as a function of the conduction band offset at the interface, for different values of the quantum well thickness. In our calculations we assume the spin is injected along z-direction and the components of the wave vector  $\mathbf{k}$  are  $k_x = 0.1\text{nm}^{-1}$  and  $k_y = 0.1\text{nm}^{-1}$ . Figure 1 shows the subband splitting for three values of the film width, namely 1.36nm, 3.3nm, and 6.5nm. Figure 1 demonstrates a complicated behavior which strongly depends on the thickness value, in contrast to the valley splitting theory in SiGe/Si/SiGe quantum wells [8], which predicts that in the case of a symmetric square well without an electric field the valley splitting is simply inversely proportional to the conduction band offset  $\Delta E_c$  at the interfaces. Figure 1 shows that for the quantum well of 1.36nm width the splitting first increases but later saturates. For the quantum well of 3.3nm width a significant reduction of the valley splitting around the conduction band offset value 1.5eV is observed. A further increase of the conduction band offset leads to an increase of the subband splitting value. For the quantum well of 3.3nm thickness the valley splitting saturates at about 0.17meV.

For the quantum well of 6.5nm width a significant reduction of the valley splitting is observed for a conduction band offset value 0.2eV. The subband splitting saturates at a value 0.04meV. Although for the values of the conduction band offset smaller than 4eV the valley splitting depends on  $\Delta E_c$ , for larger values of the conduction band offset it saturates.

The valley splitting as a function of the conduction band offset for the film of 3.3nm thickness is shown in Figure 3. Without shear strain the valley splitting is significantly reduced around the conduction band offset value of 1.5eV. For the shear strain value of 0.25% and 0.5% the sharp reduction of the conduction subbands splitting shifts to a smaller value of  $\Delta E_c$ . However the region of significant reduction is preserved even for the large shear strain value of 0.5%. The value of the valley splitting at saturation for large shear strain is considerably enhanced as compared to the unstrained case. The splitting of the lowest unprimed electron subbands as a function of the silicon film thickness for several

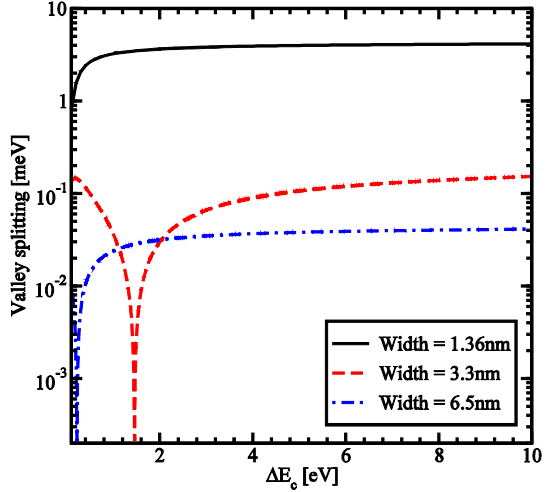


Figure 1. Splitting between the lowest unprimed electron subbands as a function of the conduction band offset at the interface for different thicknesses for  $\varepsilon_{xy}=0$ ,  $k_x = 0.1\text{nm}^{-1}$  and  $k_y = 0.1\text{nm}^{-1}$

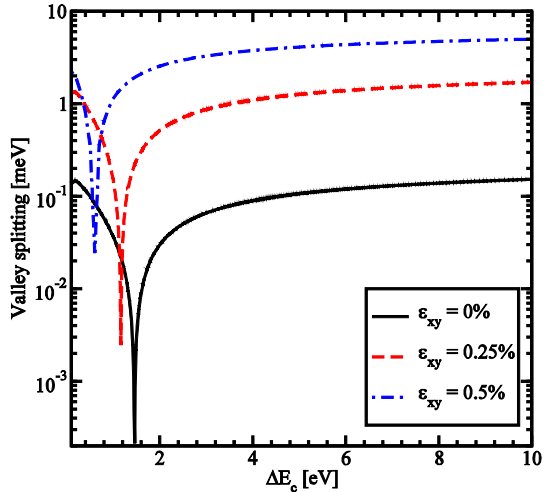


Figure 2. Valley splitting as a function of the conduction band offset for the film thickness 3.3nm for  $k_x=0.1\text{nm}^{-1}$  and  $k_y=0.1\text{nm}^{-1}$  for different shear strain values

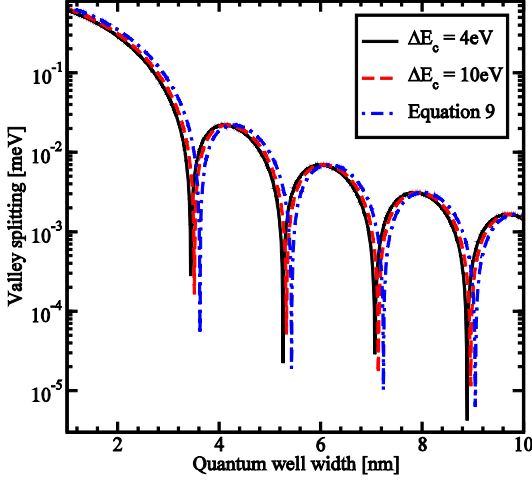


Figure 3. Splitting of the lowest unprimed electron subbands as a function of the silicon film thickness for several values of the band offset at the interface, the shear strain value is 0.05%,  $k_x = 0.1\text{nm}^{-1}$ ,  $k_y = 0.2\text{nm}^{-1}$

values of the conduction band offset at the interfaces is shown in Figure 3. The valley splitting oscillates with the film thickness increased. According to the theory [9], we generalize the equation for the valley splitting in an infinite potential square well including the spin-orbit coupling as

$$\Delta E_n = \frac{2y_n^2 B}{k_0 t \sqrt{(1-y_n^2-\eta^2)(1-y_n^2)}} \left| \sin \left( \sqrt{\frac{1-y_n^2-\eta^2}{1-y_n^2}} k_0 t \right) \right|, \quad (9)$$

with  $y_n$ ,  $\eta$ , and  $B$  defined as

$$y_n = \frac{\pi n}{k_0 t}, \quad (10)$$

$$\eta = \frac{m_l B}{\hbar^2 k_0^2}, \quad (11)$$

$$B = \sqrt{\Delta_{so}^2(k_x^2 + k_y^2) + \left(D\varepsilon_{xy} - \frac{\hbar^2 k_x k_y}{M}\right)^2}. \quad (12)$$

Here  $t$  is the film thickness. As it was shown earlier the conduction band value of 4eV provides a subband splitting value close to the saturated one. Because (9) is written for an infinite potential square well, a slight discrepancy is observed between the theoretical curve and the numerically curve calculated for the conduction band offset value 4eV in Figure 3. A large value of the conduction band offset shows better agreement between the theory and numerically obtained results.

Following (9) the results shown in Figure 1 can be understood as a consequence of zero value of the  $\left| \sin \left( \sqrt{\frac{1-y_n^2-\eta^2}{1-y_n^2}} k_0 t \right) \right|$  term. Although the conduction band offset is not included explicitly in the equation for the valley splitting, it can be taken into account through an effective film width of a finite potential well as

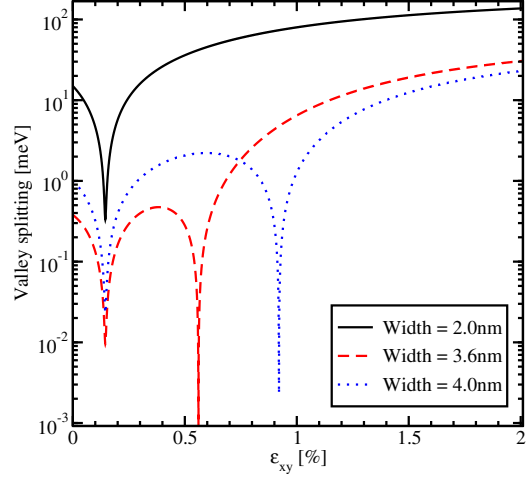


Figure 4. Intervalley splitting as a function of shear strain for different values of the well width for  $k_x = 0.25\text{nm}^{-1}$  and  $k_y = 0.25\text{nm}^{-1}$

$$t_{\text{eff}} = t + \frac{2}{\alpha}, \quad (13)$$

$$\alpha = \sqrt{\frac{2m(\Delta E_C - E)}{\hbar^2}}, \quad (14)$$

where  $E$  is the subband energy. Thus, increasing the potential barrier height leads to a decrease of the effective film thickness.

The valley splitting reductions shown in Figure 2 are also the result of the oscillating sine-like term in (9). The small increase of the shear strain leads to the decrease of the  $\sqrt{\frac{1-y_n^2-\eta^2}{1-y_n^2}}$  term. This means that in order to obtain the same conditions for larger shear strain values the effective quantum well thickness should be larger. A decrease in the conduction band offset leads precisely to such an increase of the effective thickness. Thus, the results shown in Figure 2 are in very good agreement with the theory.

Figure 4 shows the dependence of the energy splitting on strain due to stress-induced degeneracy lifting of the unprimed subband, where the in-plane wave vector  $\mathbf{k}$  components are  $k_x = 0.25\text{nm}^{-1}$  and  $k_y = 0.25\text{nm}^{-1}$ . The significant valley splitting reduction around the strain value 0.14% appears to be independent of the quantum well width. According to (9) the valley splitting is proportional to  $D\varepsilon_{xy} - \frac{\hbar^2 k_x k_y}{M}$ , and the valley splitting reduction around the shear strain value 0.14% is caused by the zero value of the  $D\varepsilon_{xy} - \frac{\hbar^2 k_x k_y}{M}$  term. At this minimum the valley splitting is determined by the spin-orbit interaction term alone. The other valley splitting minima in Figure 4 depend on the film thickness and are caused by vanishing values of the  $\left| \sin \left( \sqrt{\frac{1-y_n^2-\eta^2}{1-y_n^2}} k_0 t \right) \right|$  term.

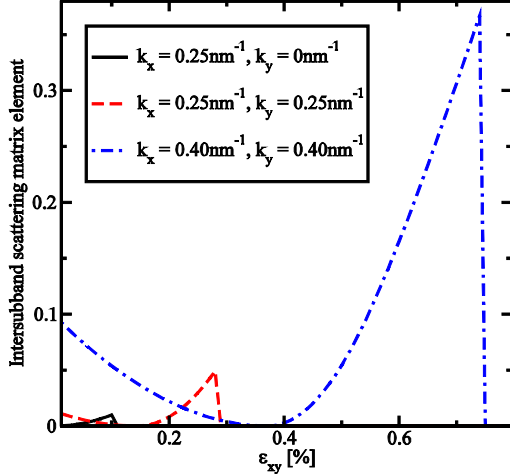


Figure 5. Intersubband scattering matrix elements normalized to the intrasubband scattering for zero strain between the states with the same spin projection for the film thickness 2nm

### B. Scattering and relaxation matrix elements calculations

The surface roughness scattering matrix elements are proportional to the square of the product of the subband function derivatives at the interface [10]. The surface roughness at the two interfaces is assumed to be equal and statistically independent. It is described by a mean and a correlation length [10]. We assume the [001] orientation for the injected spins.

The dependence on shear strain of the intersubband scattering matrix elements between the states with the same spin projection normalized to the intrasubband scattering matrix elements at zero strain is shown in Figure 5. The minimum in the intersubband scattering is achieved, when the term  $D\epsilon_{xy} - \frac{\hbar^2 k_x k_y}{M}$  is equal to zero. The intersubband scattering also vanishes, when the kinetic energy is not sufficient to have scattering states in the second subband, as shown in Figure 5.

Figure 6 shows the normalized intersubband spin relaxation matrix elements between the states with opposite spin projections as a function of shear strain for the same quantum well thickness values as in Figure 4. The valley splitting reduction determined by the zero value of the term  $D\epsilon_{xy} - \frac{\hbar^2 k_x k_y}{M}$  leads to strong mixing between the up and down spin states from the opposite valleys, and the spin relaxation matrix elements are maximal. Interestingly, other minima of the valley splitting observed for the film thicknesses 3.6nm and 4.0nm around the shear strain values 0.560% and 0.920%, respectively, do not produce any increase of the spin relaxation matrix elements. These zeroes are of a different nature due to an oscillatory dependence of the valley splitting on the film width (9) and thus they do not lead to a strong spin-up and spin-down states mixing. At the same time we observe that increasing

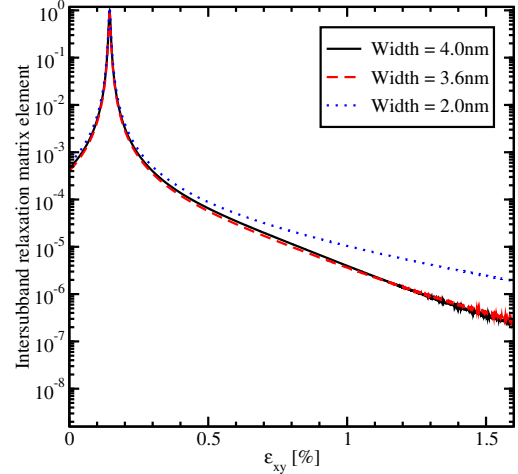


Figure 6. Intervalley spin relaxation matrix elements normalized to intravalley scattering at zero strain a function of shear strain for different values of the well width for  $k_x = 0.25\text{nm}^{-1}$  and  $k_y = 0.25\text{nm}^{-1}$

shear strain leads to a significant decrease of the spin relaxation matrix elements for all film thicknesses considered.

### IV. CONCLUSION

By generalizing the effective  $\mathbf{k} \cdot \mathbf{p}$  Hamiltonian for the conduction band in silicon to include the spin-orbit interaction effects we were able to investigate the energy splitting of the lowest electron unprimed subband in thin silicon films as function of shear strain, film thickness, band offset, and spin-orbit interaction. We have shown that the valley degeneracy is caused by two different mechanisms, one is caused by the zeroes of the  $\left| \sin\left(\sqrt{\frac{1-y_n^2-\eta^2}{1-y_n^2}} k_0 t\right) \right|$  term, while the second one, which is the critical one for the spin relaxation matrix elements, by  $D\epsilon_{xy} = \frac{\hbar^2 k_x k_y}{M}$ . We have shown that shear strain can significantly reduce spin relaxation.

### ACKNOWLEDGMENT

This work is supported by the European Research Council through the grant #247056 MOSILSPIN.

### REFERENCES

- [1] S. Sugahara and J. Nitta, Proc. of the IEEE, 98(12), 2124–2154, 2010.
- [2] S. Datta and B. Das, Appl. Phys. Lett., 56, 665, 1990.
- [3] J. Li, I. Appelbaum, Phys. Rev. B, 84, 165318, 2011.
- [4] Y. Song, H. Dery, Phys. Rev. B, 86, 085201 (2012).
- [5] G.L. Bir, G.E. Pikus, Symmetry and Strain-induced Effects in Semiconductors, J. Wiley & Sons, New York/Toronto, 1974.
- [6] V. Sverdlov, Strain-induced Effects in Advanced MOSFETs, Springer, 2011.
- [7] P. Li, H. Dery, Phys. Rev. Lett., 107, 107203, 2011.
- [8] M. Friesen, S. Chutia, C. Tahan, S.N. Coppersmith, “Valley splitting theory of SiGe/Si/SiGe quantum wells”, Physical Review B, 75, 115318, 2007.
- [9] V. Sverdlov et al., J. Comput. Electronics, 8, 3–4, 2009.
- [10] M. Fischetti et al., J. Appl. Phys., 94, 1079, 2003.